



Joule Heating and Spin-Transfer Torque Investigated on the Atomic Scale Using a Spin-Polarized Scanning Tunneling Microscope

S. Krause,* G. Herzog, A. Schlenhoff, A. Sonntag, and R. Wiesendanger

*Institute of Applied Physics and Microstructure Research Center, University of Hamburg,
Jungiusstr. 11, 20355 Hamburg, Germany*

(Received 11 April 2011; published 27 October 2011)

The influence of a high spin-polarized tunnel current onto the switching behavior of a superparamagnetic nanoisland on a nonmagnetic substrate is investigated by means of spin-polarized scanning tunneling microscopy. A detailed lifetime analysis allows for a quantification of the effective temperature rise of the nanoisland and the modification of the activation energy barrier for magnetization reversal, thereby using the nanoisland as a local thermometer and spin-transfer torque analyzer. Both the Joule heating and spin-transfer torque are found to scale linearly with the tunnel current. The results are compared to experiments performed on lithographically fabricated magneto-tunnel junctions, revealing a very high spin-transfer torque switching efficiency in our experiments.

DOI: 10.1103/PhysRevLett.107.186601

PACS numbers: 72.25.Pn, 63.22.-m, 68.37.Ef, 82.60.-s

Reorienting the magnetization of a nanostructure by injecting a spin-polarized current is in the focus of ongoing research because of its relevance for future spintronic and magnetic memory devices. A magnetic torque exerted by a spin-polarized current can cause the magnetization to flip, as proposed theoretically [1,2] and demonstrated experimentally, for example, in lithographically fabricated magneto-tunnel junctions (MTJs) [3–5]. Recent experiments using spin-polarized scanning tunneling microscopy (SP-STM) demonstrated that this current-induced magnetization switching (CIMS), driven by Joule heating, spin-transfer torque and Oersted field, is possible even when vacuum serves as the tunnel barrier [6–8]. In contrast to lithographically fabricated MTJs, the ultimate lateral resolution of SP-STM allows for a very local observation and manipulation of atomic-scale magnets. The details of the driving microscopic processes for CIMS are still to be discovered, and one important prerequisite on this way is the possibility to separate and quantify the Joule heating and spin-transfer torque on the atomic scale.

In this Letter, we will specially utilize a superparamagnetic Fe/W(110) nanoisland to explore CIMS with SP-STM. By simultaneously observing and manipulating its switching behavior with a spin-polarized tunnel current, we separate and quantitatively determine the individual contributions of Joule heating and spin-transfer torque, with the nanoisland serving as a combined local thermometer and spin-torque analyzer. Comparing our results to experiments performed on nanopillar MTJs reveals a very high spin-transfer torque efficiency for SP-STM MTJs.

As has been shown theoretically [9,10] and verified experimentally [11], the intrinsic switching behavior of a superparamagnetic particle with uniaxial anisotropy can be described by the so-called macrospin model, as illustrated in Fig. 1(a). Here, the particle magnetization has to

overcome an energy barrier E_b to reverse its orientation. All magnetic moments inside the particle rotate coherently, thereby behaving like one giant spin, and E_b is given by the total magnetic anisotropy of the particle. The mean lifetime $\bar{\tau}$ between two consecutive switching events as a function of temperature T is then given by

$$\bar{\tau} = \frac{1}{f_0} \exp\left(\frac{E_b}{k_B T}\right), \quad (1)$$

with f_0 being the attempt frequency and k_B the Boltzmann constant. The two possible magnetization orientations are labeled state **0** and state **1**, respectively. Temperature-dependent SP-STM studies on individual Fe/W(110) nanoislands revealed that the magnetization reversal is realized by a nucleation and propagation of a domain wall rather than by a coherent rotation [12]. However, the macrospin ansatz has been shown to be adequate to describe the switching behavior as long as E_b is interpreted as

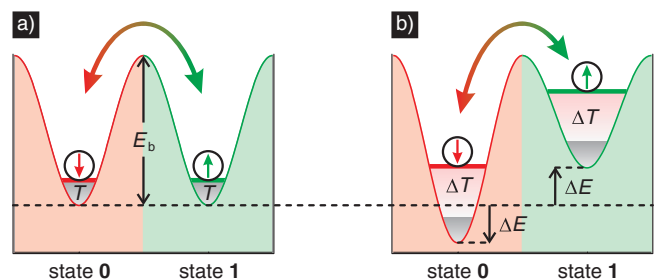


FIG. 1 (color). (a) Energy landscape schematics of a magnet with uniaxial anisotropy. Because of thermal agitation at temperature T , the magnetization may overcome the effective activation energy barrier E_b between the two states **0** and **1**. (b) Influence of a high spin-polarized current: Joule heating effectively increases T by ΔT , and spin-torque modifies E_b by $\pm\Delta E$, thereby lifting the state degeneracy and favoring switching from state **1** to state **0**.

the effective activation energy barrier for magnetization reversal [12].

CIMS experiments using SP-STM demonstrated that the intrinsic thermal switching behavior of a Fe/W(110) nanoisland is modified when passed by a high spin-polarized tunnel current I [6]: The temperature is effectively increased by ΔT due to Joule heating [13], and the activation energy barrier E_b is modified by $\pm \Delta E$ due to spin-transfer torque [14], the latter leading to an asymmetry of the state lifetimes. The situation is illustrated schematically in Fig. 1(b). There are first experimental indications for additional contributions to CIMS, like dissipation of a pure spin current [15] and thermal spin-transfer torque [16,17]. In this Letter all interactions resulting in an effective temperature rise are summarized by the term Joule heating, and all contributions leading to an asymmetry of the switching behavior are called spin-transfer torque for the sake of clarity. Oersted field contributions are found to be negligible as long as I is injected at a high symmetry point of the magnet [6]. To account for Joule heating and spin-transfer torque, we expand Eq. (1) to

$$\bar{\tau}_{0,1}(I) = \frac{1}{f_0} \exp\left(\frac{E_b \pm \Delta E(I)}{k_B[T + \Delta T(I)]}\right), \quad (2)$$

where $\bar{\tau}_0(I)$ and $\bar{\tau}_1(I)$ are the I -dependent mean lifetimes of state **0** and state **1**, respectively.

In order to quantify $\Delta T(I)$ and $\Delta E(I)$, the switching behavior of an individual nanoisland has been investigated using SP-STM at elevated I . The experiments were performed in an ultrahigh vacuum system that is equipped with a homebuilt spin-polarized scanning tunneling microscope for variable temperatures. Within our experimental setup, the entire microscope including the tip is cooled to minimize the thermal drift between tip and sample. To exclude any unwanted dipolar tip-sample interaction, anti-ferromagnetic Cr coated W tips were used which are sensitive to the in-plane component of the sample magnetization [18,19]. A W(110) single crystal serves as substrate for our experiments. Its preparation is described in detail in Ref. [20]. Evaporating 0.14 atomic layers of iron onto the substrate held at room temperature leads to the formation of pseudomorphically grown monolayer nanoislands consisting of about 30–150 atoms [12]. At a temperature of 50.6 K, these nanoislands are found to switch their magnetization frequently due to thermal agitation [12].

The differential conductance dI/dU between tip and sample is measured adding a small ac modulation voltage ($U_{\text{mod}} = 40$ mV, $f_{\text{mod}} = 4.333$ kHz) to the sample bias and detecting the resulting modulation of I by lock-in technique. Here, the spin-dependent contribution to the dI/dU signal scales with the cosine of the angle between the magnetization directions of the tip and sample [19]. Hence, positioning the tip stationary above a sample and measuring dI/dU as a function of time t allows

for recording the temporal evolution of the sample magnetization.

The $dI/dU(t)$ signal recorded above an individual Fe/W(110) nanoisland exhibits a telegraphic noise, reflecting the magnetization switching between two configurations with respect to the stable tip magnetization. As a convention, a low (high) signal is attributed to the nanoisland being in the magnetic state **0** (**1**). To extract the state-dependent mean lifetimes $\bar{\tau}_0$ and $\bar{\tau}_1$ from the telegraphic signal, every state lifetime τ_0 and τ_1 between two consecutive switching events has been determined. Traces with at least 1500 switching events have been evaluated for sake of a good statistics. Fitting the respective histograms of τ_0 and τ_1 with an exponential decay results in the mean lifetimes $\bar{\tau}_0$ and $\bar{\tau}_1$. To determine the current-dependent mean lifetimes, $\bar{\tau}_0$ and $\bar{\tau}_1$ have been evaluated for various values of I between 2 and 800 nA at a fixed bias voltage of $U = -200$ mV. The results are plotted in Fig. 2(a). As has been shown before, an overall tendency of decreasing lifetime and increasing state lifetime asymmetry towards high I is clearly visible [6].

Combining Eqs. (1) and (2) allows for the determination of the temperature rise $\Delta T(I)$ due to Joule heating and the energy splitting $\Delta E(I)$ due to spin-transfer torque:

$$\Delta T(I) = \left(\frac{1}{T} + \frac{k_B}{2E_b} \ln \frac{\bar{\tau}_0(I)\bar{\tau}_1(I)}{\bar{\tau}^2}\right)^{-1} - T, \quad (3)$$

$$\Delta E(I) = \frac{k_B[T + \Delta T(I)]}{2} \ln \frac{\bar{\tau}_0(I)}{\bar{\tau}_1(I)}, \quad (4)$$

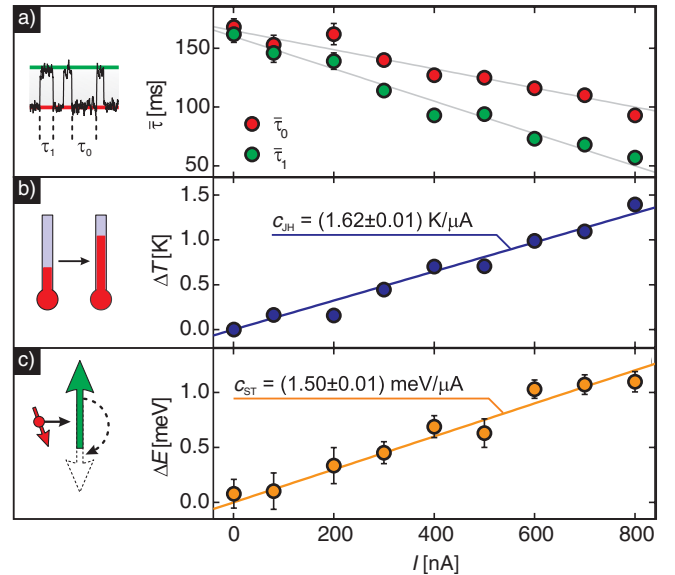


FIG. 2 (color). Tunnel current dependence of the (a) mean lifetimes $\bar{\tau}_0$ and $\bar{\tau}_1$ (gray lines are guides for the eye), (b) effective island temperature increase ΔT and (c) energy barrier modification ΔE . Error bars indicate SD. Linear fittings yield the coefficients c_{JH} and c_{ST} . $U = -200$ mV, $T = 50.6$ K.

where $\bar{\tau}$ is the intrinsic mean lifetime determined at $I = 2$ nA. To deduce E_b , the mean lifetimes of the intrinsic thermal switching behavior have been determined at two different temperatures and low I , resulting in $E_b = (133 \pm 4)$ meV.

The results for $\Delta T_{\text{JH}}(I)$ are plotted in Fig. 2(b). Obviously, the temperature rises linearly as a function of I . This is consistent with an experimental study of heat generation between an STM tip and a metallic sample, demonstrating that the Joule heat dissipated in the sample scales linearly with I at constant bias voltage U [13]. Fitting the data with $\Delta T(I) = c_{\text{JH}}I$ yields $c_{\text{JH}} = (1.62 \pm 0.01)$ K/ μA , where c_{JH} is introduced as the differential heating coefficient of the MTJ. Consequently, the thermal energy of the nanoisland is increased by up to 3% of $k_B T$. Because of the Arrhenius-like switching behavior, this tiny temperature increase already considerably reduces the mean lifetimes by a factor of 2.

It has been shown experimentally that the thermal conductivity of a nanocontact is drastically reduced with respect to its bulk value due to phonon confinement [21]. Since Fe/W(110) nanoislands are strongly confined vertically as well as laterally, we expect a very local heat dissipation within the nanoisland due to phonon generation by the tunneling electrons, with the temperature of the substrate remaining almost unaffected. Likewise, variations of the temperature within the nanoisland are assumed to be negligible, although the spot of tunnel current injection is confined to a cross-sectional area given by the typical SP-STM lateral resolution of 5 Å [22].

Many experiments addressing Joule heating were performed on lithographically fabricated nanopillar MTJs. Here, a typical temperature increase of about 2 K/(mW μm^{-2}) is deduced on μm size junctions [23]. However, the layered nature of these devices strongly hinders a direct investigation of the local Joule heating inside an MTJ. For example, imperfections may create so-called hot spots where the local current density and therefore also the local temperature rise may increase by up to 13 times the average value [23]. Our SP-STM experiments allow for a very local and quantitative investigation of Joule heating on the atomic scale on well-defined structures. The Fe nanoisland has a base area of about 5.5 nm², resulting in a temperature increase of 44 K/(mW μm^{-2}). This value is in accordance with STM experiments performed on Co/Cu(111) nanoislands, where the temperature increase has been roughly estimated to be 30–300 K/(mW μm^{-2}) [24].

In Fig. 2(c), the results for the spin-transfer torque contribution $\Delta E(I)$ are plotted. As for $\Delta T(I)$, a linear scaling behavior with I is observed. This finding is in accordance with theoretical studies on the thermally assisted magnetization reversal in the presence of a spin-transfer torque [14]. Fitting the data with $\Delta E = c_{\text{ST}}I$

results in $c_{\text{ST}} = (1.50 \pm 0.01)$ meV/ μA , with c_{ST} being introduced as the differential modification of E_b .

To compare the spin-transfer torque in our SP-STM experiments to that in nanopillar MTJs, we calculate the so-called torkance [25]

$$\frac{d\Gamma}{dU}(I) = \frac{d\Gamma}{dI} \frac{dI}{dU}(I) = \frac{\hbar}{2e} \eta \frac{dI}{dU}(I). \quad (5)$$

Here, η is the tunnel current spin-polarization. It can be determined from the MTJ work function ϕ and the tip-sample distance variation Δz between parallel and antiparallel configuration of tip and sample magnetization at closed feedback loop [26]. From $I(z)$ spectroscopy experiments we deduce $\phi = 3.12$ eV, resulting in $\eta = 0.07$.

The experimental results for the torkance are shown in Fig. 3(a). In contrast to CIMS experiments performed on nanopillar devices at low bias [5], the torkance is not constant. This is reasonable, since in our experiments high tunnel currents are realized by reducing the distance between the SP-STM tip and the nanoisland, thereby increasing the tunnel conductivity. We find $dI/dU(I) = 0.01 \mu\text{S/nA} \times I$, resulting in $d\Gamma/dU(800 \text{ nA}) = 5.6 \times 10^{-4} \hbar/(2e) \text{ k}\Omega^{-1}$ for the maximum tunnel current of $I = 800$ nA. This value is by 4 orders of magnitude lower than in experiments performed on lithographically fabricated MTJs, yielding $d\Gamma/dU \approx 0.1 \hbar/(2e) \text{ k}\Omega^{-1}$ [5]. However, the magnetic moment that has to be switched in an atomic-scale nanoisland is much lower than in a nanopillar structure. From the topography map shown in Fig. 3(c), we estimate the nanoisland consisting of about 78 atoms. Given a magnetic moment of 2.79 Bohr magneton per Fe atom [27], this results in a total magnetic moment of $m = 2 \times 10^{-21}$ A/m². The nanopillar MTJ of Ref. [5] has a total magnetic moment of $m = 1 \times 10^{-17}$ A/m². To provide a measure of the switching efficiency, we relate the torkance to the magnetic moment by defining the spin-transfer torque viscosity ν_{ST} :

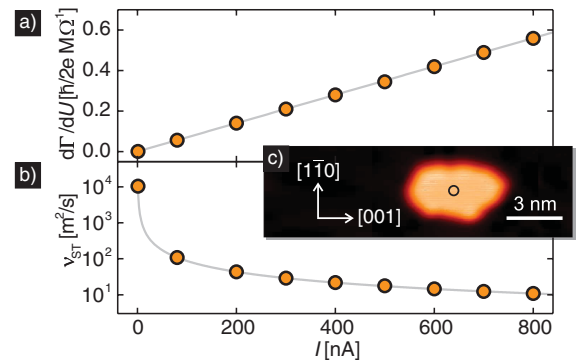


FIG. 3 (color). Experimentally determined tunnel current dependence of the (a) torkance $d\Gamma/dU$ and (b) spin-transfer torque viscosity ν_{ST} . Gray lines are guides to the eye. (c) Topography map of the nanoisland. The point of current injection is marked by a circle.

$$\nu_{\text{ST}}(I) := m \left(\frac{d\Gamma}{dU}(I) \right)^{-1}. \quad (6)$$

Here, a low viscosity implies a high impact of the spin-transfer torque onto m . As can be seen from Fig. 3(b), $\nu_{\text{ST}} \approx 10^4 \text{ m}^2/\text{s}$ at low I . With increasing I , the spin-transfer torque viscosity drops by about 3 orders of magnitude, indicating a dramatic increase of the switching efficiency. At $I = 800 \text{ nA}$, $\nu_{\text{ST}} = 11 \text{ m}^2/\text{s}$. For the nanopillar MTJ of Ref. [5], $\nu_{\text{ST}} = 217 \text{ m}^2/\text{s}$. Consequently, the spin-transfer torque impact onto m within our SP-STM experiments is by a factor of 20 higher than in experiments performed on typical nanopillar MTJs. For a fictitious spin-polarization of $\eta = 1$, the spin-transfer torque viscosity will drop down by another order of magnitude, with $\nu_{\text{ST}} \leq 1 \text{ m}^2/\text{s}$ for $I = 800 \text{ nA}$.

As discussed before, in contrast to experiments on nanopillar MTJs where the current is generally considered to be homogeneously distributed, the area of spin-polarized tunnel current injection in our studies is confined to a spot diameter of 5 \AA [22], resulting in a local current density of up to $4 \times 10^8 \text{ A/cm}^2$. Hence, only a fractional part of the nanoisland will be directly affected by the spin-polarized tunnel current. For smaller nanoislands with sizes being comparable to that of the current injection spot, we expect a further decrease of ν_{ST} , since then the whole nanomagnet is affected by the spin-transfer torque.

In summary, we performed an experimental study on an individual Fe/W(110) nanoisland using SP-STM to quantitatively determine the contributions of Joule heating and spin-transfer torque as a function of the spin-polarized tunnel current. A detailed lifetime analysis reveals that both the effective temperature rise as well as the modification of the effective activation energy barrier scale linearly with the tunnel current. Comparing the temperature increase and the spin-transfer torque to that in lithographically fabricated MTJs in terms of torque and spin-transfer torque viscosity, we find a very high switching efficiency in our SP-STM experiments. The presented concept of investigating the current-dependent switching behavior of a single superparamagnetic nanoisland by means of SP-STM opens the perspective for a variety of new experiments. For example, the influence of single impurities on the switching efficiency are not accessible in experiments using nanopillar MTJs. Our studies allow for a detailed investigation of Joule heat generation and spin-transfer torque switching on the atomic scale, thereby providing new insight into the details of CIMS.

Financial support from the Grants No. SFB 668-B4 and No. GrK 1286 of the Deutsche Forschungsgemeinschaft, from the ERC Advanced Grant FUIRORE and from the Cluster of Excellence NANOSPINTRONICS is gratefully acknowledged.

*skrause@physnet.uni-hamburg.de

- [1] J. C. Slonczewski, *J. Magn. Magn. Mater.* **159**, L1 (1996).
- [2] L. Berger, *Phys. Rev. B* **54**, 9353 (1996).
- [3] Y. Huai, F. Albert, P. Nguyen, M. Pakala, and T. Valet, *Appl. Phys. Lett.* **84**, 3118 (2004).
- [4] G. D. Fuchs, N. C. Emley, I. N. Krivorotov, P. M. Braganca, E. M. Ryan, S. I. Kiselev, J. C. Sankey, D. C. Ralph, R. A. Buhrman, and J. A. Katine, *Appl. Phys. Lett.* **85**, 1205 (2004).
- [5] J. C. Sankey, Y.-T. Cui, J. Z. Sun, J. C. Slonczewski, R. A. Buhrman, and D. C. Ralph, *Nature Phys.* **4**, 67 (2007).
- [6] S. Krause, L. Berbil-Bautista, G. Herzog, M. Bode, and R. Wiesendanger, *Science* **317**, 1537 (2007).
- [7] G. Herzog, S. Krause, and R. Wiesendanger, *Appl. Phys. Lett.* **96**, 102505 (2010).
- [8] S. Loth, M. Etzkorn, C. P. Lutz, D. M. Eigler, and A. J. Heinrich, *Science* **329**, 1628 (2010).
- [9] M. L. Néel, *Ann. Geophys.* **5**, 99 (1949).
- [10] W. F. Brown, *Phys. Rev.* **130**, 1677 (1963).
- [11] W. Wernsdorfer, E. B. Orozco, K. Hasselbach, A. Benoit, B. Barbara, N. Demoncey, A. Loiseau, H. Pascard, and D. Maily, *Phys. Rev. Lett.* **78**, 1791 (1997).
- [12] S. Krause, G. Herzog, T. Stapelfeldt, L. Berbil-Bautista, M. Bode, E. Y. Vedmedenko, and R. Wiesendanger, *Phys. Rev. Lett.* **103**, 127202 (2009).
- [13] I. Bat'ko and M. Bat'ková, *Eur. Phys. J. Appl. Phys.* **31**, 191 (2005).
- [14] Z. Li and S. Zhang, *Phys. Rev. B* **69**, 134416 (2004).
- [15] A. A. Tulapurkar and Y. Suzuki, *Phys. Rev. B* **83**, 012401 (2011).
- [16] M. Hatami, G. E. W. Bauer, Q. Zhang, and P. J. Kelly, *Phys. Rev. Lett.* **99**, 066603 (2007).
- [17] H. Yu, S. Granville, D. P. Yu, and J.-P. Ansermet, *Phys. Rev. Lett.* **104**, 146601 (2010).
- [18] A. Kubetzka, M. Bode, O. Pietzsch, and R. Wiesendanger, *Phys. Rev. Lett.* **88**, 057201 (2002).
- [19] A. Wachowiak, J. Wiebe, M. Bode, O. Pietzsch, M. Morgenstern, and R. Wiesendanger, *Science* **298**, 577 (2002).
- [20] M. Bode, S. Krause, L. Berbil-Bautista, S. Heinze, and R. Wiesendanger, *Surf. Sci.* **601**, 3308 (2007).
- [21] D. Li, Y. Wu, P. Kim, L. Shi, P. Yang, and A. Majumdar, *Appl. Phys. Lett.* **83**, 2934 (2003).
- [22] J. Tersoff and D. R. Hamann, *Phys. Rev. Lett.* **50**, 1998 (1983).
- [23] R. C. Sousa, I. L. Prejbeanu, D. Stanescu, B. Rodmacq, O. Redon, B. Dieny, J. Wang, and P. P. Freitas, *J. Appl. Phys.* **95**, 6783 (2004).
- [24] N. Néel, J. Kröger, and R. Berndt, *Appl. Phys. Lett.* **95**, 203103 (2009).
- [25] J. C. Slonczewski and J. Z. Sun, *J. Magn. Magn. Mater.* **310**, 169 (2007).
- [26] R. Wiesendanger, H. J. Güntherodt, G. Güntherodt, R. J. Gambino, and R. Ruf, *Phys. Rev. Lett.* **65**, 247 (1990).
- [27] J. Hauschild, H. J. Elmers, and U. Gradmann, *Phys. Rev. B* **57**, R677 (1998).